A NUMERICAL EVALUATION OF PREDICTION ACCURACY OF CO_2 ABSORBER MODEL FOR VARIOUS REACTION RATE COEFFICIENTS

by

Sung-Min SHIM [a], ***Sang-Jin LEE*** [b], ***and Woo-Seung KIM*** [c*]

[a] Department of Mechanical Engineering, Hanyang University, Seoul, Korea South
[b] Energy Research Department, STX Institute of Technology, Seoul, Korea South
[c] Department of Mechanical Engineering, Hanyang University, Seoul, Korea South

Original scientific paper
DOI: 10.2298/TSCI120202126S

The performance of the CO_2 absorber column using monoethanolamine (MEA) solution as chemical solvent are predicted by a 1-D rate based model in the present study. 1-D mass and heat balance equations of vapor and liquid phase are coupled with interfacial mass transfer model and vapor-liquid equilibrium model. The two-film theory is used to estimate the mass transfer between the vapor and liquid film. Chemical reactions in MEA-CO_2-H_2O system are considered to predict the equilibrium pressure of CO_2 in the MEA solution. The mathematical and reaction kinetics models used in this work are calculated by using in-house code. The numerical results are validated in the comparison of simulation results with experimental and simulation data given in the literature. The performance of CO_2 absorber column is evaluated by the 1-D rate based model using various reaction rate coefficients suggested by various researchers. When the rate of liquid to gas mass flow rate is about 8.3, 6.6, 4.5, and 3.1, the error of CO_2 loading and the CO_2 removal efficiency using the reaction rate coefficients of Aboudheir et al. is within about 4.9% and 5.2%, respectively. Therefore, the reaction rate coefficient suggested by Aboudheir et al. among the various reaction rate coefficients used in this study is appropriate to predict the performance of CO_2 absorber column using MEA solution.

Key words: *CO_2 capture and storage, 1-D rate-based model, kinetics, reaction rate, mass transfer, monoethanolamine*

Introduction

The major cause of global warming is CO_2 released into atmosphere by consuming fossil fuels. CO_2 emissions are mainly generated by large CO_2 sources such as fossil fuel power plant, cement plant, steel plant, and refinery. Therefore, effective strategies such as carbon capture and storage (CCS) are essentially required to reduce the CO_2 emission from a large CO_2 source.

The CO_2 capture technologies are usually divided into three main-categories: post-combustion, pre-combustion, and oxy-fuel combustion. Among these technologies, the post-

* Corresponding author; e-mail: wskim@hanyang.ac.kr

combustion technology is effective at low CO_2 concentration about 3~15% and includes absorption, adsorption, membrane, and cryogenics. Koukouzas *et al.* conducted a case study to evaluate the possibilities for CCS including CO_2 capture, transportation and storage in the Komotini NGCC power plant [1]. In the post-combustion technology, chemical absorption technology using an aqueous solution of chemical base is used most widely for the CO_2 capture in fossil fuel power plants, since this has the advantage that it can be retrofitted to existing plant. In chemical absorption, the mainly used solution is aqueous alkanolamine solutions, such as monoethanolamine (MEA), diethanolamine (DEA), methyldiethanolamine (MDEA) and *etc*. Among these solutions, MEA is the most commonly used solvent for CO_2 capture [2]. In addition, a investigation for CO_2 looping cycles using CaO-based sorbent was performed by Manovic *et al.* [3].

The widely used approaches for modeling and design of a reactive absorption process are the equilibrium-based approach and the rate-based approach to predict the behavior of CO_2 absorber column. The equilibrium-based approach subdivides the absorber column into several segments and assumes that the vapor and liquid phase reach equilibrium at each stage [4]. The rate-based approach is called as non-equilibrium approach and calculates the mass and heat transfer between the vapor and liquid phase [5]. Based on these approaches, various absorber column models at different levels of complexity were developed by previous researchers. Kenig *et al.* [6] classified various forms of models into 5 levels according to complexity for mass transfer and reaction model. In CO_2 absorber column using aqueous alkanolamine solution, vapor and liquid phase equilibrium is rarely achieved at each stage, because CO_2 absorption process is a rate-based-controlled phenomenon [7]. Therefore, the rate-based approach is more appropriate for modeling the CO_2 absorber column than the equilibrium-based approach.

The investigations for the chemical reactions of MEA-CO_2-H_2O system were widely conducted by various researchers. Hikita *et al.* [8], Versteeg *et al.* [9], Horng *et al.* [10] investigated the reaction rate for MEA-CO_2-H_2O system at very narrow ranges of temperature. Freguia [11] adjusted the reaction rate coefficient suggested by Hikita *et al.* [8] and Kvamsdal *et al.* [12] modified the latter even further. At high CO_2 loaded aqueous MEA solution, Aboudheir *et al.* [13] developed a termolecular kinetics model for MEA-CO_2-H_2O system over the temperature range from 293 K to 333 K. Vaidya *et al.* [14] summarized the previous researches for the reaction kinetics of CO_2 absorption into aqueous MEA solution.

In Lawal *et al.* [15], a dynamic absorber column model was developed based on the rate-based approach. In this model, it was assumed that the chemical reactions are at equilibrium for considering the mass transfer. Lawal *et al.* [15] results showed that the rich solvent loading and the CO_2 absorption level were in good agreement with the experimental data obtained by Dugas [16]. On the other hand, this model showed poor prediction for the liquid temperature profile in the absorber column. In Kvamsdal *et al.* [17], a dynamic model for absorber column was developed by using enhancement factor for consideration of rate-based mass transfer. In this work, the height of packing and the flue gas flow rate were adjusted in gPROMS to obtain the similar CO_2 absorption efficiency as measured in the experiment.

In the present work, a rate-based model is used to predict the performance of CO_2 absorber column. 1-D mass and heat balance equations for vapor and liquid phase are used to obtain the distribution of each species concentration and temperature along the height of column. These governing equations are coupled with the mass transfer through vapor-liquid interface and the chemical reaction for CO_2 absorption into aqueous MEA solution. The mass

transfer across vapor-liquid interface can be explained by using the two-film theory. To consider the chemical reaction for CO_2 absorption into aqueous MEA solution, an enhancement factor is used. It is assumed that the chemical reaction only occurs in liquid film and the equilibrium stage is attained at the bulk liquid region. To consider the rate-based mass transfer, the following chemical reactions are considered: ionization of water, dissociation of dissolved CO_2 through carbonic acid, dissociation of bicarbonate, carbamate reversion to bicarbonate, dissociation of protonated MEA and overall reaction of MEA and CO_2. Equilibrium constant proposed by Edwards *et al.* [18] and Kent *et al.* [19] are applied for the vapor-liquid equilibrium model.

In this work, various types of reaction rate coefficient of the CO_2/aqueous MEA reaction are applied to the rate based model. The rate based model used in this study is validated by comparing the simulation results with experimental and simulation results given in the literature. Then the proper reaction rate coefficient is chosen for predicting the temperature profile and CO_2 removal efficiency of CO_2 absorber column.

Modeling

This section describes the absorber model based on the rate based approach for predicting the phenomena that happen in the CO_2 absorber column using aqueous MEA solution. Figure 1 shows a schematic of CO_2 absorber column and a control volume used in the present study. It is assumed that the CO_2 absorber column is a packed column and vapor phase species are CO_2, MEA, H_2O and N_2, while the liquid phase species are CO_2, MEA, H_2O, N_2, $MEAH^+$, HCO_3^-, OH^-, $MEACOO^-$ and H_3O^+. CO_2 rich gas enters at the bottom and flows upward through the packing while the CO_2 lean MEA solution is uniformly distributed at the top of the packing and flows downward. It is assumed that the each control volume is composed of bulk vapor phase, bulk liquid phase, vapor film and liquid film, then the mass transfer is occurred through the interface between vapor and liquid film.

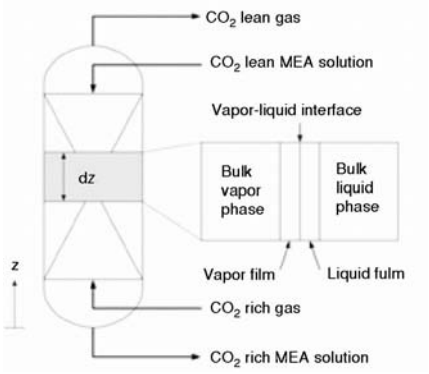

Figure 1. Schematic of CO_2 absorber column and a control volume

Mass and heat balance equations

The partial differential equations (PDE) are used to simulate the time and spatial behavior of concentration and temperature of the CO_2 absorption process in a plug flow reactor. Mass and heat balance equations of vapor and liquid phase are summarized below [17].

The total mass balance equations for the vapor and liquid phases are, respectively:

$$\varepsilon_{\mathrm{v}} \frac{\mathrm{d}F_{\mathrm{v}}}{\mathrm{d}t} = -u_{\mathrm{v}} \frac{\partial F_{\mathrm{v}}}{\partial z} + u_{\mathrm{v}} a_{\mathrm{w}} \sum N_i \tag{1}$$

$$\varepsilon_{\mathrm{l}} \frac{\mathrm{d}F_{\mathrm{l}}}{\mathrm{d}t} = -u_{\mathrm{l}} \frac{\partial F_{\mathrm{l}}}{\partial z} - u_{\mathrm{l}} a_{\mathrm{w}} \sum N_i \tag{2}$$

where ε_v and ε_l are the vapor and liquid holdup, F_v and F_l – the molar flow rate for the vapor and liquid phase, u_v and u_l are vapor and liquid velocities, a_w is the effective interfacial area of packing, and N_i – the mass flux of component i.

The species mass balance equations for the vapor and liquid phases are, respectively:

$$\varepsilon_v \frac{dC_i^v}{dt} = -u_v \frac{\partial C_i^v}{\partial z} + a_w N_i \tag{3}$$

$$\varepsilon_l \frac{dC_i^l}{dt} = -u_l \frac{\partial C_i^l}{\partial z} - a_w N_i \tag{4}$$

where C_i^v and C_i^l are the concentration component i for the vapor and liquid phase.

The heat balance equations for the vapor and liquid phases are, respectively:

$$\varepsilon_v \frac{dT_v}{dt} = -u_v \frac{\partial T_v}{\partial z} + \frac{a_w}{\sum (C_i C_{p,i})_v} h_{v/l} (T_l - T_v) \tag{5}$$

$$\varepsilon_l \frac{dT_l}{dt} = -u_l \frac{\partial T_l}{\partial z} - \frac{a_w}{\sum (C_i C_{p,i})_l} [h_{v/l}(T_l - T_v) - \Delta H_r N_{CO_2} - \Delta H_{vap} N_{H_2O}] \tag{6}$$

where T_v and T_l are the vapor and liquid temperature, $C_{p,i}$ is the specific heat capacity of component i, $h_{v/l}$ – the interfacial heat transfer coefficient, ΔH_r – the absorption heat of CO_2, and ΔH_{vap} – the vaporization heat of H_2O.

Interfacial mass transfer model

In this paper, the flux of CO_2, MEA, and H_2O is defined as follows:

$$N_i = K_{ov,i}(P_i^{eq,*} - P_i^v) \tag{7}$$

where $K_{ov,i}$ is the overall mass transfer coefficient, $P_i^{eq,*}$ – the equilibrium partial pressure of component i in the liquid phase, and P_i^v – the partial pressure of component i in the vapor phase.

In this study, the mass transfer in the vapor-liquid interface is described by the two-film model. In two film theory, the overall mass transfer coefficient is defined in terms of the resistance to mass transfer in the vapor and liquid film. In case of MEA and H_2O, the resistance to mass transfer in the liquid film can be ignored since the MEA and H_2O concentrations are high in the liquid phase. Therefore, the overall mass transfer coefficient of MEA and H_2O is expressed by:

$$K_{ov,i} = \frac{k_i^v}{RT_v} \tag{8}$$

where k_i^v is the vapor side mass transfer coefficient, and R – the gas constant.

The overall mass transfer coefficient of CO_2 is given by:

$$\frac{1}{K_{ov,CO_2}} = \frac{RT_v}{k_{CO_2}^v} + \frac{H_{CO_2}}{k_{CO_2}^l E_{CO_2}} \tag{9}$$

where H_{CO_2} is the Henry's law constant of CO_2, $k_{CO_2}^l$ – the mass transfer coefficient of liquid film and E_{CO_2} – the enhancement factor of CO_2 absorption. The first and the second term of right hand side of eq. (9) represent the resistance to mass transfer in gas and liquid

phase, respectively. The correlations given by Onda *et al.* [20] for vapor and liquid side mass transfer coefficient are applied in this model.

In this work, the pseudo first order enhancement factor is used for CO_2 absorption in MEA solution. The enhancement factor is defined as follows:

$$E_{CO_2} = \frac{\sqrt{k_{r,CO_2} C^*_{MEA} D_{CO_2}}}{k^l_{CO_2}} \tag{10}$$

where k_{r,CO_2} is the reaction rate coefficient for the reaction of CO_2 with the MEA solution, C^*_{MEA} – the free MEA concentration in liquid, and D_{CO_2} – the diffusion coefficient of CO_2 in MEA solution.

Vapor-liquid equilibrium model

For the prediction of the mass transfer in the vapor-liquid interface, it is necessary to estimate the equilibrium pressure of CO_2 and the liquid concentration of all components existing in the aqueous MEA solution. Therefore, the vapor-liquid equilibrium model is adopted for analysis of kinetics in MEA-CO_2-H_2O system. The chemical reactions considered are as follows: [13]

Ionization of water:

$$2H_2O \xleftrightarrow{K_1} OH^- + H_3O^+ \tag{11}$$

Dissociation of dissolved CO_2 through carbonic acid:

$$CO_2 + 2H_2O \xleftrightarrow{K_2} HCO_3^- + H_3O^+ \tag{12}$$

Dissociation of bicarbonate:

$$HCO_3^- + H_2O \xleftrightarrow{K_3} CO_3^{2-} + H_3O^+ \tag{13}$$

Carbamate reversion to bicarbonate:

$$RNHCOO^- + H_2O \xleftrightarrow{K_4} RNH_2 + HCO_3^- \tag{14}$$

Dissociation of protonated MEA:

$$RNH_3^+ + H_2O \xleftrightarrow{K_5} RNH_2 + H_3O^+ \tag{15}$$

The liquid concentration of all species shown in the chemical reactions and their equilibrium partial pressure of species can be obtained by solving the equations [13]:

MEA balance:

$$[RNH_2] + [RNH_3^+] + [RNHCOO^-] = [RNH_2]_0 \tag{16}$$

Carbon balance:

$$[CO_2] + [HCO_3^-] + [CO_3^{2-}] + [RNHCOO^-] = \alpha[RNH_2]_0 \tag{17}$$

Charge balance:

$$[RNH_3^+] + [H_3O^+] = [HCO_3^-] + [OH^-] + 2[CO_3^{2-}] + [RNHCOO^-] \tag{18}$$

Equilibrium constants:

$$K_1 = [OH^-][H_3O^+] \tag{19}$$

$$K_2 = [\mathrm{HCO_3^-}][\mathrm{H_3O^+}]/[\mathrm{CO_2}] \tag{20}$$

$$K_3 = [\mathrm{CO_3^{2-}}][\mathrm{H_3O^+}]/[\mathrm{HCO_3^-}] \tag{21}$$

$$K_4 = [\mathrm{RNH_2}][\mathrm{HCO_3^-}]/[\mathrm{RNHCOO^-}] \tag{22}$$

$$K_5 = [\mathrm{RNH_2}][\mathrm{H_3O^+}]/[\mathrm{RNH_3^+}] \tag{23}$$

The equilibrium pressure of each species:

$$P_{\mathrm{CO_2}}^{\mathrm{eq},*} = H_{\mathrm{E,CO_2}} C_{\mathrm{CO_2}}^{*} \tag{24}$$

$$P_i^{\mathrm{eq},*} = x_i P_i \tag{25}$$

where α is the CO_2 loading, $C_{\mathrm{CO_2}}^{*}$ – the free CO_2 concentration at equilibrium, x_i – the free MEA and H_2O mole fraction, and P_i – the partial pressure of MEA and H_2O. Table 1 shows the equilibrium constants used in this study.

Table 1 Equilibrium constants used in the VLE model [18, 19]

Reaction	a_1	a_2	a_3	Reference
12	–13445.90	–22.4773	140.93200	Edwards *et al.* [18]
13	–12092.10	–36.7816	235.48200	Edwards *et al.* [18]
14	–12431.70	–35.4819	220.06700	Edwards *et al.* [18]
15	–3090.83	0.0000	6.69425	Kent *et al.* [19]
16	–5851.11	0.0000	–3.36360	Kent *et al.*[19]
$K_{\mathrm{eq}} = \exp(a_1/T + a_2 \ln T + a_3)$				

Model validation

Numerical method

The algebraic and partial differential equations were calculated by in-house code. The Broyden's method is applied for solving the nonlinear equation. The method of backward finite differences over a uniform grid of 200 elements is used to discretize the spatial variables.

Validation of vapor-liquid equilibrium model

For validation of the equilibrium constants used in this study, the present results were compared with the numerical data predicted by Liu *et al.* [21]. The CO_2 loading was varied from 0 to 1 in a 2.5 M MEA solution at 313 K. The concentration of each component was shown in fig. 2. The present results are in good agreement with those of Liu *et al.* [21]. With increasing CO_2 loading in the aqueous solution, MEA concentration is decreased. Otherwise the concentrations of main product, such as $[RNH_3^+]$, $[RNHCOO^-]$, and $[HCO_3^-]$ are increased because of the reaction between CO_2 and MEA. When the CO_2 loading is over 0.5, the concentration of $[RNH_2]$ is increased because of carbamate reversion to bicarbonate. However, $[RNH_2]$ is rapidly protonated by reverse reaction of dissociation of protonated MEA and then the concentration of $[RNH_3^+]$ is gradually increased with increasing CO_2 loading. In fig. 3, partial pressure of CO_2 at the vapor-liquid interface is also validated by comparing the present result with experimental data [22]. At 30 wt.% MEA concentration, the

numerical result of CO_2 partial pressure for solution temperature of 40 °C, 60 °C, 80 °C, 100 °C, and 120 °C indicates a very good representation of experimental results. Consequently, vapor-liquid equilibrium model used in this work is appropriate for the prediction of the mass transfer in the vapor-liquid interface.

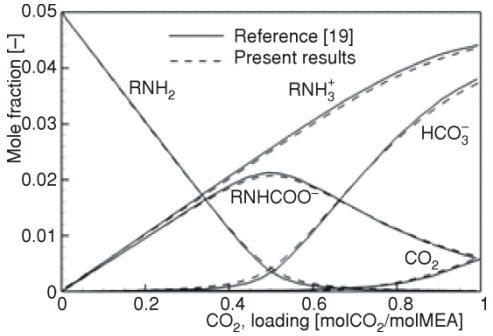

Figure 2. Liquid phase concentration in 2.5 M MEA solution with respect to CO_2 loading at 313 K

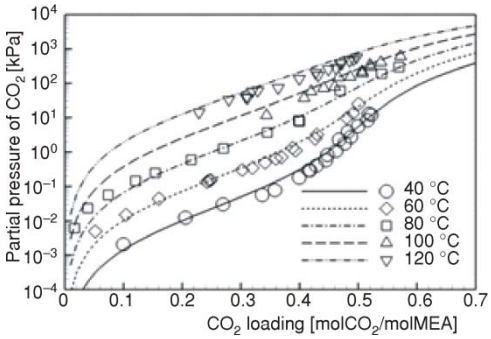

Figure 3. Partial pressure of CO_2 at 30 wt.% MEA solution with respect to CO_2 loading (line: numerical result, symbol: experimental result [22])

Validation of the rate-based model

In this study, the data from Dugas [16] is used for validation of the rate based model. Table 2 shows the information of absorber column and packing material. The CO_2 absorber column of the pilot plant is a packed column with a diameter of 0.427 m, a total height of 11.1 m and total packing height of 6.1 m. The packing in the absorber column is IMTP–40 with a void fraction of 0.98, a nominal packing size of 0.04 m and a specific surface of 154 m^2/m^3.

Table 2. Absorber column and packing material data [16]

Absorber column	
Column inside diameter [m]	0.427
Column height [m]	11.1
Packing material data	
Packing type	IMTP–40
Height of packing [m]	6.1
Void fraction [–]	0.98
Nominal packing size [m]	0.04
Specific surface area [m^{-1}]	153

Table 3 shows the operating conditions of absorber column used to validate the present model. The reaction rate of Aboudheir *et al.* [13] is applied for validation of the rate based model used in this work.

Table 3 Operating conditions of absorber column for Case 47 [16]

Flue gas	Temperature [K]	332.38
	Flow rate [m^3s^{-1}]	509.60
	CO_2 fraction	0.1841
Lean MEA	Temperature [K]	313.37
	Flow rate [m^3s^{-1}]	1.81
	CO_2 loading	0.281

Figure 4 shows the liquid temperature profiles of the experimental data the present simulation result. The present result shows that there is no temperature gradient at the top, middle, and bottom of the absorber column. In the region it is assumed that the reaction of

CO_2 absorption into MEA solution is not occurred because the packing does not exist. The liquid temperature profiles in the present study are in good agreement with Dugas's [16] result, except bottom, and top of column. At the bottom and top of column, the interfacial contact area between liquid and vapor phase is sharply decreased than the packed region, since there is no packing. The possibility that the actually measured temperature is the vapor phase temperature is high. Therefore, the numerical and experimental results show the big discrepancy at the bottom and top of column.

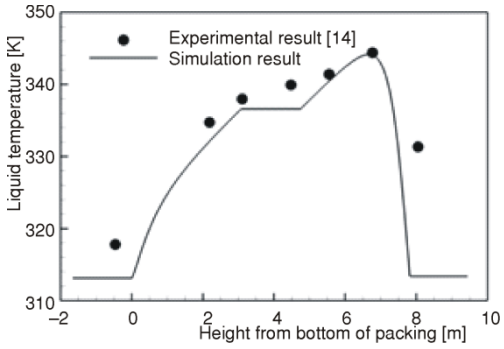

Figure 4. Comparison of the simulation result and experiment [16]

Table 4 shows the comparison of the experimental and the simulation result for the rich CO_2 loading and CO_2 removal efficiency. The present results show that the deviation of rich CO_2 loading and CO_2 removal efficiency is about 5.0% and 7.8%, respectively. Therefore, the analysis model used in this work shows good agreement with the experimental results for the temperature profile, CO_2 loading and CO_2 removal efficiency of CO_2 absorber column.

Table 4. Comparison of the experiment [16] and simulation result

	Experiment	This work	
		Simulation	% dev.
Rich CO_2 loading [mol/mol]	0.539	0.512	5.0
CO_2 removal efficiency [%]	69.0	63.6	7.8

Results and discussions

The comparison of simulation results using various reaction rate coefficients suggested by Hikita *et al.* [8], Versteeg *et al.* [9], Horng *et al.* [10], Freguia [11], Kvamsdal *et al.* [12], and Aboudheir *et al.* [13] with the pilot-scale experimental data from Dugas [16] is performed in the present study. Table 5 presents the reaction rate coefficients between CO_2 and MEA as suggested by previous literatures [8-13]. Table 6 indicates the operating conditions of absorber column. Four cases which has 8.3, 6.6, 4.5, and 3.1 of *L/G*, respectively, were selected to choose the appropriate reaction rate coefficient covering over all experimental range.

Table 5. Reaction rate coefficients of the CO_2/aqueous MEA reaction system

Reference	Reaction rate coefficient [$m^3mol^{-1}s^{-1}$]
Hikita *et al.* [8]	$9.770\times10^7\exp(-4955.0/T)$
Versteeg *et al.* [9]	$4.440\times10^8\exp(-5400.0/T)$
Horng *et al.* [10]	$3.014\times10^8\exp(-5376.2/T)$
Freguia [11]	$3.200\times10^3\exp(-1348.0/T)$
Kvamsdal *et al.* [12]	$2.950\times10^3\exp(-1500.0/T)$
Aboudheir *et al.* [13]	$4600\exp(-4412/T)[RNH_2] + 4.55\times\exp(-3287/T)[CO_2]$

Table 6. Operating conditions of absorber column

		Case 25	Case 39	Case 41	Case 43
Flue gas	Temperature [K]	328.12	328.39	325.50	326.66
	Flow rate [m^3s^{-1}]	679.23	680.96	678.96	679.04
	CO_2 fraction	0.173	0.169	0.171	0.170
Lean MEA	Temperature [K]	313.11	313.34	313.34	313.17
	Flow rate [m^3s^{-1}]	6.254	4.994	3.402	2.360
	CO_2 loading	0.278	0.228	0.235	0.231
Liquid to gas mass flow ratio [–]		8.3	6.6	4.5	3.1

Figures 5 to 8 show the variations of the temperature in the liquid phase with respect to the reaction rate coefficients for Case 25, Case 39, Case 41, and Case 43, respectively. In Case 25, the temperature profile of present result using Aboudheir *et al.* [13] shows a good agreement with experimental data within the error of less than 2 K. However, the others used in the present study show the big difference between numerical and experimental results [16]. In Case 39, the temperature profiles of numerical results are similar with Case 25. The peak temperature of MEA solution is 7 K higher than that of Case 25. The height of peak temperature is shifted around 0.6 m from bottom, since the liquid flow rate is decreased.

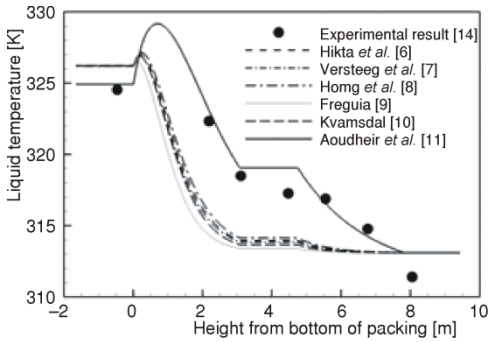

Figure 5. Variations of the temperature in the liquid phase with respect to the reaction rate coefficients in Case 25

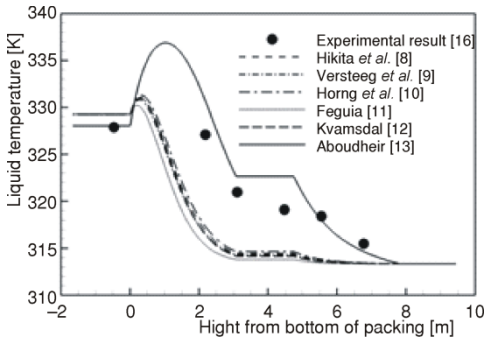

Figure 6. Variations of the temperature in the liquid phase with respect to the reaction rate coefficients in Case 39

Under the conditions of Case 41, the reaction rate coefficients used in this study show good agreement with experimental results [16]. Among these results, the reaction rate coefficient of Aboudheir *et al.* [13] show higher prediction accuracy than any others. In Case 43, the reaction rate coefficient of Aboudheir *et al.* [13] is also well agreement with experimental data [16]. The simulation results using the reaction rate coefficients except Aboudheir *et al.* [13] show 3 K higher peak temperature than experimental result [16] because CO_2 absorption into MEA solution is over estimated. The simulation results using the reaction rate coefficient suggested by Aboudheir *et al.* [13] are compared with the experimental data [16] as shown in tab. 7. The deviation of the CO_2 loading and the CO_2 removal efficiency using the reaction rate coefficients of Aboudheir *et al.* [13] are below about 4.9% and 5.2%, respectively. This results show that the reaction rate coefficient suggested by Aboudheir *et al.* is appropriate to predict the performance of CO_2 absorber column using aqueous MEA solution. It is ascribed to more accurate reaction rate coeffcient obtained by Aboudheir *et al.* [13] in wide range experiments of MEA concentration of 3~9 mol/L, CO_2 loading of 0.1~0.49 and liquid temperature of 293~333 K. The data from the experiments allow that the detailed

variation of CO_2 absorption rate as a function of MEA concentration can be considered in the modified reaction rate coefficient suggested by Aboudheir *et al.* [13]. Hence, the results show that the reaction rate coefficient suggested by Aboudheir *et al.* [13] is the most appropriate one among candidates considered in the present study to predict the performance of CO_2 absorber column using aqueous MEA solution.

Table 7. Comparison of experiments [16] and simulation results

Case	Rich CO_2 loading [–]			CO_2 removal efficiency [%]		
	Exp.	Sim	% dev.	Exp.	Sim	% dev.
25	0.386	0.403	4.404	93	92.140	0.925
39	0.367	0.385	4.904	94	94.492	0.523
41	0.433	0.449	3.695	87	86.412	0.675
43	0.491	0.498	1.425	72	75.712	5.155

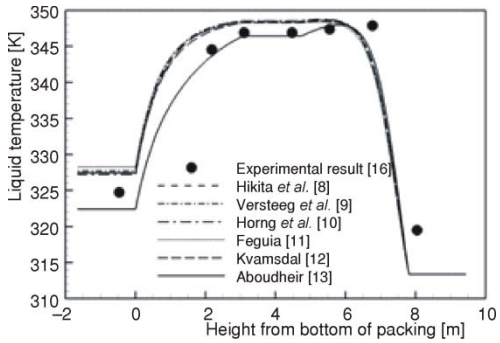

Figure 7. Variations of the temperature in the liquid phase with respect to the reaction rate coefficients in Case 41

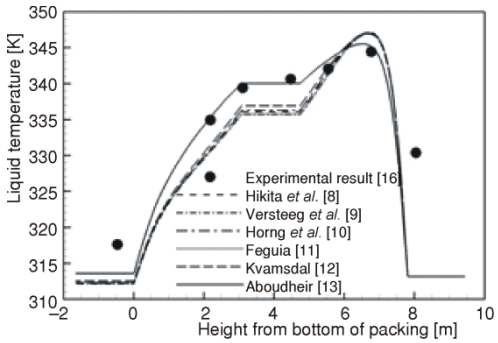

Figure 8. Variations of the temperature in the liquid phase with respect to the reaction rate coefficients in Case 43

Conclusions

In the present study, the reaction rate coefficients suggested by Hikita *et al.* [8], Versteeg *et al.* [9], Horng *et al.* [10], Freguia [11], Kvamsdal *et al.* [12] and Aboudheir *et al.* [13] are applied to the present model. Then the liquid temperature profile of the present numerical result with respect to the reaction rate coefficients is compared with that of experimental data [16]. Among 48 experiments with various conditions conducted by Dugas [16], four cases which cover almost range of the ratio of liquid to gas mass flow rate are selected for comparison of the reaction rate coefficients. The rate of liquid to gas mass flow rate of these cases is about 8.3, 6.6, 4.5, and 3.1, respectively. The liquid temperature profile using the reaction rate coefficient suggested by Aboudheir *et al.* [11] show the best result in the various reaction rate coefficients used in this study for Case 25, Case 39, Case 41, and Case 43 among candidates. The error of CO_2 loading and the CO_2 removal efficiency using the reaction rate coefficients of Aboudheir *et al.* [13] is within about 4.9% and 5.2%, respectively. It is shown that the reaction rate coefficient suggested by Aboudheir *et al.* is appropriate to predict the performance of CO_2 absorber column using aqueous MEA solution due to more accurate data obtained by Aboudheir *et al.* [13] from experiments in various range than the previous literatures.

Acknowledgment

This research was supported by the Basic Science Research Program through the National Research Foundation of Korea (NRF), funded by the Ministry of Education, Science and Technology (2011-0017220).

Nomenclature

a_w – effective interfacial area, [m^{-1}]
C – concentration, [$molm^{-3}$]
C_p – heat capacity, [$Jmol^{-1}K^{-1}$]
D – diffusivity, [m^2s^{-1}]
E – enhancement factor, [–]
H – Henry's law constant, [$m^3kPamol^{-1}$]
ΔH_r – heat of reaction, [$Jmol^{-1}$]
ΔH_{vap} – heat of vaporization, [$Jmol^{-1}$]
h – specific interfacial heat transfer coefficient, [$Wm^{-2}K^{-1}$]
K_{eq} – equilibrium constant, [mol^2L^{-6}],[$molL^{-3}$]
K_{ov} – overall mass transfer coefficient, [$molm^{-2}kPa^{-1}s^{-1}$]
k – vapor and liquid side mass transfer coefficient, [ms^{-1}]
k_r – reaction rate coefficient, [$m^3mol^{-1}s^{-1}$]
N – molar flux, [$molm^{-2}s^{-1}$]
P – pressure, [kPa]
R – gas constant, [$Jmol^{-1}K^{-1}$]
T – temperature, [K]
t – time, [s]
u – velocity, [ms^{-1}]
z – height, [m]

Greek symbols

α – CO_2 loading, [–]
ε – holdup, [–]

Subscripts

i – component
l – liquid
v – vapor

Superscripts

* – interface value of variable
eq – equlibrium
l – liquid
v – vapor

References

[1] Koukouzas, N., *et al.,* CO_2 Capture and Storage in Greece: a Case Study from Komotini NGCC Power Plant, *Thermal Science, 10* (2006), 3, pp. 71-80
[2] Akanksha Pant, K. K., Sirvastava, V. K., Carbon Dioxide Absorption into Mono-ethanolamine in a Continuous Film Contactor, *Chemical Engineering Journal, 133* (2007), 1-3, pp. 229-237
[3] Manovic, V., Anthony, E. J., Improvement of CaO-Based Sorbent Performance for CO_2 Looping Cycles, *Thermal Science, 13* (2009), 1, pp. 89-104
[4] Taylor, R., Krishna, R., Multicomponent Mass Transfer, John Wiley and Sons, Inc., New York, USA, 1993
[5] Noeres, C., Kenig, E. Y., Gorak, A., Modelling of Reactive Separation Processes: Reactive Absorption and Reactive Distillation, *Chemical Engineering Progress*, *42* (2003), 3, pp. 157-178
[6] Kenig, E. Y., Schneider, R., Gorak, A., Reactive Absorption: Optimal Process Design via Optimal Modelling, *Chemical Engineering Science, 56* (2001), 2, pp 343-350
[7] Schneider, R., Kenig, E. Y., Gorak, A., Dynamic Modelling of Reactive Absorption with the Maxwell-Stefan Approach, *Transactions of IChemE, 77* (1999), 7, pp. 633-638
[8] Hikita, H., *et al.,* The Kinetics of Reactions of Carbon Dioxide with Monoethanolamine, Diethanolamine and Triethanolamine by a Rapid Mixing Method, *Chemical Engineering Journal*, *13* (1977), 1, pp. 7-12
[9] Versteeg, G. F., van Dijck, L. A., van Swaaij, P. M., On the Kinetics between CO_2 and Alkanolamines both in Aqueous an Non-Aqueous Solutions, A review, *Chemical Engineering Communications, 144* (1996), pp. 113-158
[10] Horng, S., Li, M., Kinetics of Absorption of Carbon Dioxide into Aqueous Solutions of Mono-Ethanolamine + Tri-Ethanolamine, *Industrial and Engineering Chemistry Research, 41* (2002), 2, pp. 257-266
[11] Freguia, S., Modeling of CO_2 Removal from Flue Gases with Monoethanolamine, M. Sc. thesis, University of Texas, Austin, Tex., USA, 2002

[12] Kvamsdal, H. M., Rochelle, G. T., Effects of Temperature in CO_2 Absorption from Fue Gas by Aqueous Mono-Ethanolamine, *Industrial and Engineering Chemistry Research*, *43* (2008), 3, pp. 867-875
[13] Aboudheir, A., Tontiwachwuthikul, P., Chakma, A., Idem, R., Kinetics of the Reactive Absorption of Carbon Dioxide in High CO_2-loaded, Concentrated Aqueous Mono-ethanolamine Solutions, *Chemical Engineering Science*, *58* (2003), 23-24, pp. 5195-5210
[14] Vaidya, P. D., Kenig, E. Y., CO_2-Alkanolamine Reaction Kinetics: a Review of Recent Studies, *Chemical Engineering and Technology, 30* (2007), 11, pp. 1467-1474
[15] Lawal, A., *et al*., Dynamic Modelling of CO_2 Absorption for Post Combustion Capture in Coal-Fired Power Plants, *Fuel, 88* (2009), 12, pp. 2455-2462
[16] Dugas, R. E., Pilot Plant Study of Carbon Dioxide Capture by Aqueous Mono-ethanolamine, M. Sc. thesis, University of Texas, Austin, Tex., USA, 2006
[17] Kvamsdal, H. M., Jakobsen, J. P., Hoff, K. A., Dynamic Modeling and Simulation of a CO_2 Absorber Column for Post-Combustion CO_2 Capture, *Chemical Engineering and Processing, 48* (2009), 1, pp. 135-144
[18] Edwards, J. T., *et al*., Vapor-Liquid Equilibria in Multicomponent Aqueous Solutions of Volatile Weak Electrolytes, *American Institute of Chemical Engineers Journal, 24* (1978), 6, pp. 966-976
[19] Kent, R. L., Eisenberg, B., Better Data for Amine Treating, *Hydrocarbon Processing, 55* (1976), 2, pp. 87-90
[20] Onda, K., Takeuchi, H., Okumuto, Y., Mass Transfer Coefficients between Gas and Liquid Phases in Packed Columns*, Journal of Chemical Engineering Japan*, *1* (1968), pp. 56-62
[21] Liu, Y., Zhang, L., Watanasiri, S., Representing Vapor-Liquid Equilibrium for an Aqueous MEA-CO_2 System using the Electrolyte Nonrandom-Two-Liquid Model, *Industrial Engineering Chemical Research*, *38* (1999), 5, pp. 2080-2090
[22] Ugochukwu, E. A., *et al.,* Equilibrium in the H_2O-MEA-CO_2 System: New Data and Modeling, 1st Post Combustion Capture Conference, Abu Dhabi, United Arab Emirates, 2011

Paper submitted: February 2, 2012
Paper revised: June 2, 2012
Paper accepted: June 13, 2012